ELSEVIER

Nuclear Instruments and Methods in Physics Research B 173 (2001) 503–515

NIM B
Beam Interactions with Materials & Atoms

www.elsevier.nl/locate/nimb

Scattering of atoms and molecules off a barium zirconate surface

S. Jans [a,1], P. Wurz [a,*], R. Schletti [a], K. Brüning [b], K. Sekar [b,2], W. Heiland [b], J. Quinn [c], R.E. Leuchtner [c]

[a] *University of Bern, Physikalisches Institut, Sidlerstrasse 5, CH-3012 Bern, Switzerland*
[b] *Universität Osnabrück, Fachbereich Physik, Barbarastrasse 7, D-49069 Osnabrück, Germany*
[c] *University of New Hampshire, EOS, Durham, NH 03824, USA*

Received 28 March 2000; received in revised form 17 August 2000

Abstract

Neutral particle imaging in the low-energy range will, when employed in future spacecraft missions, potentially contribute to enlarging our knowledge about the origin and evolution of our universe. The main difficulty for a neutral particle detector in this energy range is that the incoming neutrals must first be ionized such that they can be mass- and energy-analyzed by conventional methods. In this paper, we report on the first observation of the formation of negatively charged ions upon reflection from a barium zirconate surface. Experiments were performed at two different setups, one of them including a time-of-flight (TOF) measurement of the specularly reflected particles, the other one allows position-resolved detection. We measured high fractions (22–35%) of negative ions and no positive ions when scattering O^+, O^0, O_2^+ and O_2^0 at 500–3000 eV primary energy per atom off a $BaZrO_3$ surface. When scattering H^+, H_2^+ and H_2^0 at 300–1500 eV per atom off the $BaZrO_3$ surface, 3–5% of the particles were converted into negative ions and 2–8% into positive ions. Our results suggest a complete memory loss of the incident charge state. Scattered molecules dissociated almost completely. The mean energy loss was proportional to the incident particle energy. $BaZrO_3$ therefore meets the most important requirements for application on a space platform.

PACS: 78.70.–g; 61.18.Bn
Keywords: $BaZrO_3$; Neutral particle imaging; Particle scattering; Surface ionization

1. Introduction

Knowledge about the origin and evolution of our solar system, our galaxy, and the universe can be achieved by determining the composition of matter. The measured abundances of the elements and isotopic ratios help constrain cosmological models. The composition of our solar system

* Corresponding author. Fax: +41-31-631-44-05.
E-mail addresses: jans@dpmail.epfl.ch (S. Jans), peter.wurz@soho.unibe.ch (P. Wurz).
[1] Present address: EPFL, Department de Physique, Institute de Physique Experimentale, 1015 Lausanne-Ecublens, Switzerland. Fax: +41-21-693-3604.
[2] Present address: University of Virginia, Charlottesville, VA, USA.

0168-583X/01/$ - see front matter
PII: S0168-583X(00)00421-3

reveals interstellar matter of the proto-solar nebula some 4.5 billion years ago. A sample of the present-day galaxy with reliable observations of a number of important elemental and isotopic abundance ratios is missing.

Unlike the ionized component of the interstellar gas, which is excluded from penetrating inside the heliosphere by the solar wind plasma, the neutral component of the interstellar gas can penetrate deeply into the heliosphere and therefore, some of its components can be measured even as close to the sun as the Earth orbit. This yields direct information about the composition of the local interstellar medium. Moreover, energetic neutral particles (expected energy range is 0.1–5 keV), which are produced by charge-exchange between interstellar neutral gas and heliospheric particles can be measured. A two-dimensional image of the neutral fluxes helps infer the interaction processes between the local interstellar medium and the heliospere. We expect to detect mainly atomic particles (mainly H, He and O) since they are much more abundant than molecules in the local interstellar gas [1] or in planetary magnetospheres [2].

However, in a neutral particle detector, the incoming neutrals must first be ionized such that they can be mass-analyzed by conventional methods. Neutral particle imaging in the low-energy range requires efficient ionization methods since the expected fluxes are very small. Surface ionization was identified as the only viable ionization technique to meet the requirements concerning ionization efficiency for the energy range 10 eV–1 keV within the limitations imposed by the resources (space, weight, power, etc.) available on a satellite [3]. It was concluded that the detection efficiency should exceed 1%, should be uniform over large areas, and should exhibit good long-term stability during the mission duration. Surface ionization introduces new demands on the design of the mass spectrometer and requires the development of new analyzer elements with matched ion optical properties. An instrument meeting these demands has been described recently [4,5] and is currently operating successfully on the IMAGE satellite [2]. Surface ionization was studied extensively for low work function surfaces [6–8] with the low work function of the surfaces established by coating a typical metal with an alkali or an alkaline-earth overlayer [9,10].

Preparing such coated metal surfaces with sufficient quality and reproducibility in an instrument on a spacecraft turns out to be quite involved [11]. Thus, we focused our research on insulating surfaces [12,13], which yield reasonable results without preparation in space. These surfaces are much easier to handle than the rather involved coated tungsten surfaces, which is of great importance for an application on a spacecraft.

In the present work, we present the experimental results for the negative and positive ion fractions we obtained when scattering hydrogen and oxygen particles off a $BaZrO_3$ surface. In addition, we report on the energy loss the projectiles experience upon scattering.

2. Experimental setup

The measurements reported here were made in part at the University of Bern and in part at the University of Osnabrück. The two setups will both be described briefly. More detailed information on the experimental setups at the University of Bern and at the University of Osnabrück can be found in [13] and [14], respectively.

The investigated scattering surface was a $BaZrO_3$ film of about 20 nm thickness deposited on W(1 1 0) using the pulsed laser deposition method [15]. A KrF excimer laser (248 nm wavelength, 30 ns FWHM pulsewidth) was focused onto the $BaZrO_3$ target inside a vacuum chamber (base pressure 2×10^{-7} mbar) to provide the material to coat the W(1 1 0) crystal. Typical focal spot areas were 5×10^{-6} m^2 with an average laser pulse energy of 0.50 J/pulse. The laser was incident on the $BaZrO_3$ target at an angle of 45°. During the film growth, the substrate temperature was held constant at about 400°C and the background pressure was 0.070 mbar (oxygen). 300 laser shots of $BaZrO_3$ were deposited, resulting in 15–20 nm film thickness, and then cooled to room temperature in 1 bar of O_2. Analytical characterization of the crystal structure was performed using X-ray diffraction (XRD). Upon receipt from the vendor, the 12 mm tungsten crystal had an RMS rough-

ness of 3.3 nm, as measured by atomic force microscopy over a typical 5 μm area. After cleaning and colloidal silica polish, the RMS roughness was 0.45 nm, and following $BaZrO_3$ deposition it was 1.0 nm.

2.1. Bern experiment

The experiment ILENA at the University of Bern (see Fig. 1) consists of an ion source, a beam-guiding system, a sample stage with housing and with an alkali dispenser unit (not used for this study), and a detection unit. All these units are contained in a single vacuum chamber pumped by a turbomolecular pump. Ions are formed in an electron-impact ion source (Nier type), with the intensity of the primary ion beam of ~10 fA. Molecular ions of hydrogen and oxygen were used because they can be produced far more efficiently in this system. The ions are then deflected in a 90° cylindrical analyzer with an energy width of the ion beam at the sample of $\Delta E/E = 1\%$ (FWHM). The energy analyzer focuses the ion beam on the entrance aperture of the sample housing. Two diaphragms limit the beam size to ∅ 1 mm and the beam divergence to 1°. The impact angle of the ion beam on the conversion surface can be chosen between 90° and 0° with respect to the surface normal. The reflected beam is recorded with a two-dimensional position-sensitive MCP detector with a viewing angle of ±12.5° in azimuthal and ±12.5° in polar direction. A retarding potential analyzer (RPA) consisting of three grids is mounted in front of the MCP detector. The detector unit, including the RPA, is shielded electrostatically and can be rotated independently from the converter surface around the same axis. The outer grids of the RPA are grounded to shield the inner grid, which can be biased to suppress positive ions. An additional grid in front of the MCP detector at negative potential with respect to the MCP detector serves to reject secondary electrons originating from the preceding grids and the converter surface. The MCP detector may be floated at a high negative voltage with respect to the converter surface to eliminate negative particles.

After baking out the vacuum chamber, a residual gas pressure of 5×10^{-8} mbar is achieved.

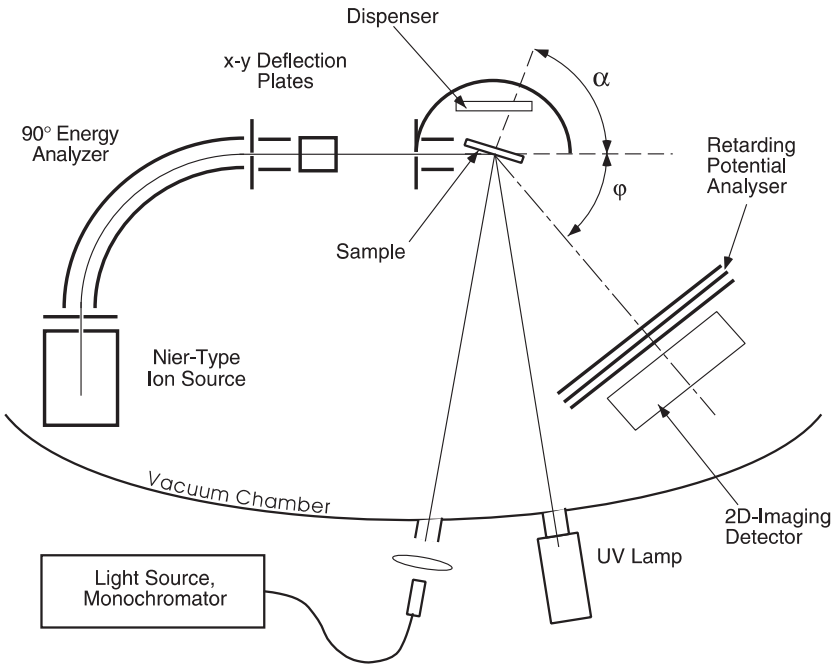

Fig. 1. Experimental setup at the University of Bern.

During operation, the pressure may rise into the low 10^{-7} mbar range as a result of the test gas leaking into the ion source chamber. The sample can be heated in order to remove adsorbates from the surface.

2.2. Osnabrück experiment

The experimental system JUSO at the University of Osnabrück (Fig. 2) is a UHV system with a base pressure in the low 10^{-9} mbar range. Primary ions are extracted from an ion plasma source and mass-analyzed by a 90° sector field magnet. With an electric deflection system in front of the analyzing magnet, the primary beam can be pulsed to allow time-of-flight (TOF) measurements. The scattering surface is mounted onto a three-axis manipulator equipped with electron beam heating. A thermocouple is used for temperature control. Downstream from the target, the TOF tube is mounted at a fixed scattering angle of 10°. Scattered ions are separated from scattered neutral particles by a postacceleration voltage. In the detector, a microsphere plate is used. The angle aperture for detection is 1.2°.

Neutral primary particles are produced by neutralization of the primary ion beam in a gas cell which is placed behind the analyzing magnet and in front of the target chamber. We almost never observed any recoil atoms in the TOF spectra.

3. Results

Fig. 3 shows the TOF spectrum for a 787 eV primary H_2^+ beam reflected from the $BaZrO_3$ surface at a scattering angle of 10° and postaccelerated with −1200 V. The charged particles therefore appear at smaller TOFs, corresponding to their higher energies. We could not identify a H_2^0 peak, which would appear at the same TOF as the H^0 peak, but would be narrower and thus clearly distinguishable [16,17]. As can be seen from the small H_2^+ peak also, almost all molecular ions dissociated. We used molecular neutral and positive primary hydrogen beams in the energy range 550–3000 eV. The fraction of detected H_2^+ molecules in the scattered beam was always less than 1% for primary energies below 1000 eV and for higher energies, no molecular ion peak appeared in the TOF spectrum. When applying a positive postacceleration voltage, only the H^0 and the H^- peak were observed.

Molecular neutral and positive primary oxygen beams from 1000 to 3100 eV were produced. Fig. 4

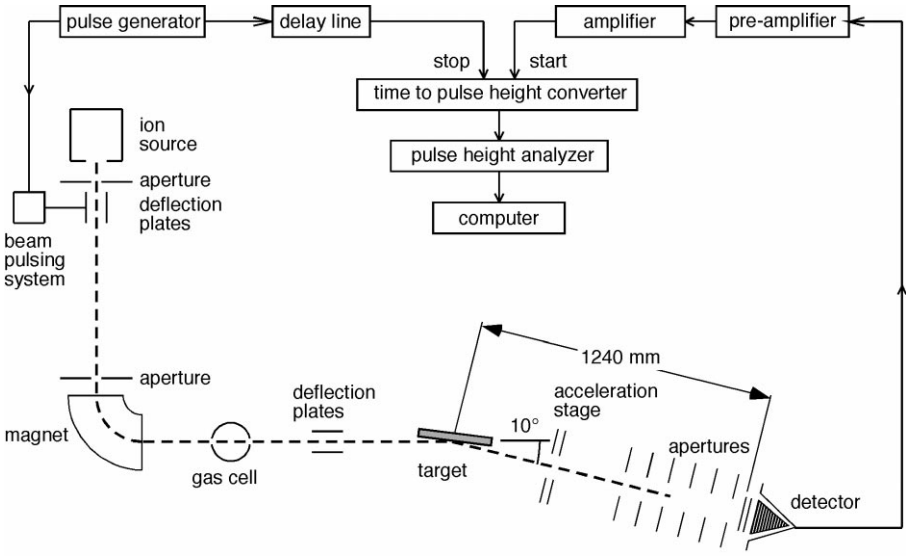

Fig. 2. Experimental setup at the University of Osnabrück.

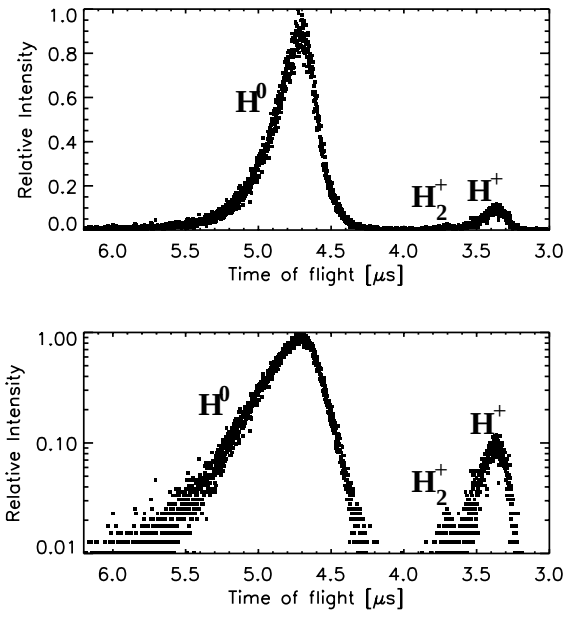

Fig. 3. TOF spectrum for primary H_2^+ ions reflected from a $BaZrO_3$ surface at an incoming angle of about 5° (as measured from the surface plane) at 787 eV energy and a −1200 V postacceleration voltage. Upper panel: linear scale; lower panel: logarithmic scale. Few surviving H_2^+ molecules could be detected.

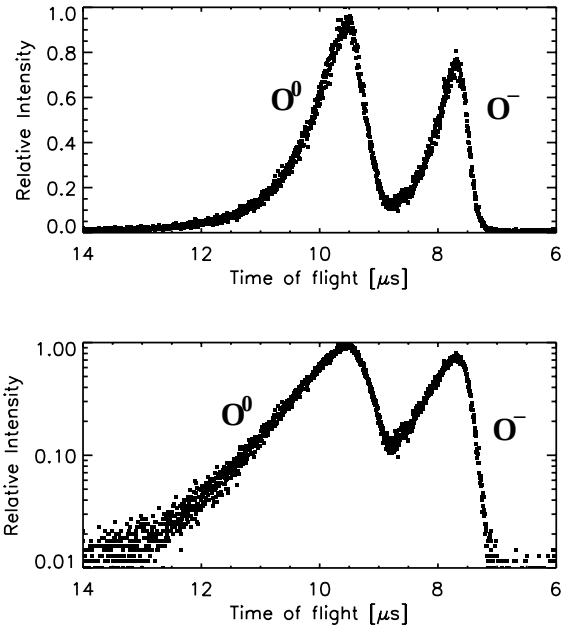

Fig. 4. TOF spectrum for primary O_2^+ ions reflected from a $BaZrO_3$ surface at an incoming angle of about 5° (as measured from the surface plane) at 3082 eV energy and a +2000 V postacceleration voltage.

shows a TOF spectrum for a 3082 eV primary O_2^+ beam scattered off the $BaZrO_3$ surface and accelerated with +2000 V. Only the O^0 and O^- peaks can be identified in Fig. 4. For a negative postacceleration voltage, the detected beam seemed to consist only of neutral atoms. We never found any molecular peak in the TOF spectra, which means that all oxygen molecules dissociated during the scattering event on the $BaZrO_3$ surface.

We also scattered atomic hydrogen (950–1500 eV) and oxygen (700–3050 eV) primary particles. From the recorded TOF spectra, we calculated the mean energy loss upon reflection from the $BaZrO_3$ surface for all primary particles. These results are shown in Figs. 5 and 6 for hydrogen and oxygen, respectively. It can be seen from Figs. 5 and 6 that the energy loss is the same for neutral and positively charged primary molecules and atoms when plotted versus primary energy per atom. For hydrogen, the mean energy loss amounts to 12% and does not seem to depend on the outgoing particle charge state or energy. For oxygen, we found a slight but significant difference in the energy loss of neutral and negatively charged atoms after reflection from the surface. The neutral atoms and the negative ions lost 15% and 18%, respectively, of their primary energy.

Fig. 7 depicts the fits to the measured energy distributions of the outgoing particles for a 1450 eV primary H_2^0 beam reflected from $BaZrO_3$ at a scattering angle of 10°. The thin lines are the H^+ and H^- distributions scaled to the height of the H^0 curve. After reflection, the energy distributions were essentially the same for neutral, positively and negatively charged hydrogen particles. This corresponds well to the results of the mean energy loss, which came out the same for all primary hydrogen particles.

By contrast, for oxygen, the energy distributions were different for outgoing neutral and negatively charged particles. This can be seen from Fig. 8, which shows the fits to the measured energy distributions of the outgoing particles for an

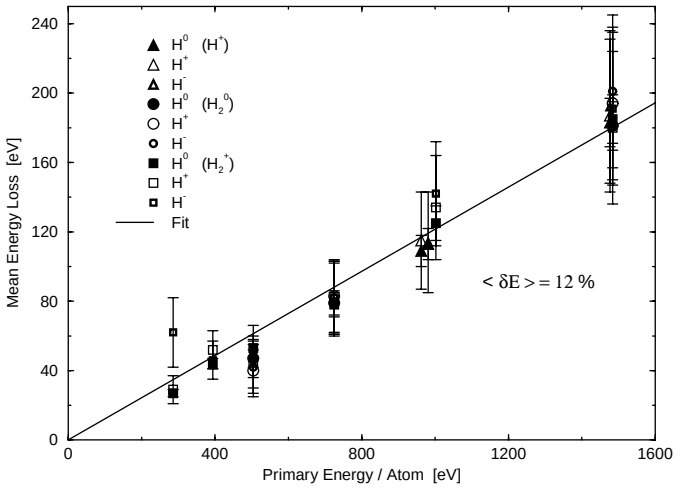

Fig. 5. Primary H^+ (triangles), H_2^0 (circles) and H_2^+ (squares) at 300–1500 eV per atom were scattered off a $BaZrO_3$ surface at 10° scattering angle. The figure shows the mean energy loss measured for outgoing H^0 (filled symbols), H^+ (thin open symbols) and H^- (thick open symbols). The energy loss is the same for charged and neutral particles and also independent of the primary particles used. The line indicates a fit through all data points.

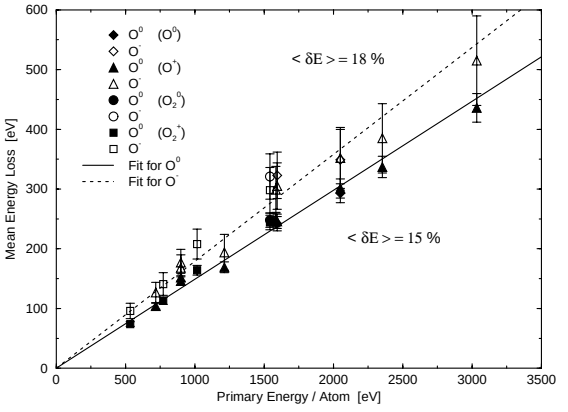

Fig. 6. Primary O^0 (diamonds), O^+ (triangles), O_2^0 (circles) and O_2^+ (squares) at 500–3000 eV per atom were scattered off a $BaZrO_3$ surface at 10° scattering angle. The figure shows the mean energy loss measured for outgoing O^0 (filled symbols) and O^- (open symbols). Negative ions lose more energy than neutrals, but the energy loss does not depend on the primary particle type. The solid and dashed lines are fits to the data points of neutrals and negative ions, respectively.

incoming 3033 eV O^+ beam. The thin O^- line is scaled to the height of the O^0 curve. The shape of the energy distribution of the negative oxygen atoms does not correspond with that of the neutrals.

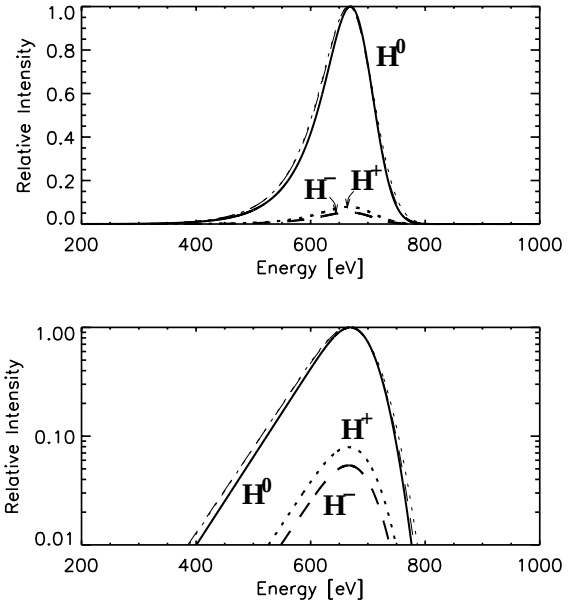

Fig. 7. Fits to the measured energy distributions for neutral (solid line), positive (pointed lines) and negative (dashed lines) hydrogen particles after reflection for a H_2^0 primary beam at 1450 eV impinging on a $BaZrO_3$ surface at an incoming angle of about 5°, as measured from the surface plane. The thin lines are the positive and negative ion distributions scaled to match the neutral atom distribution. Within the experimental uncertainty, the curves are the same.

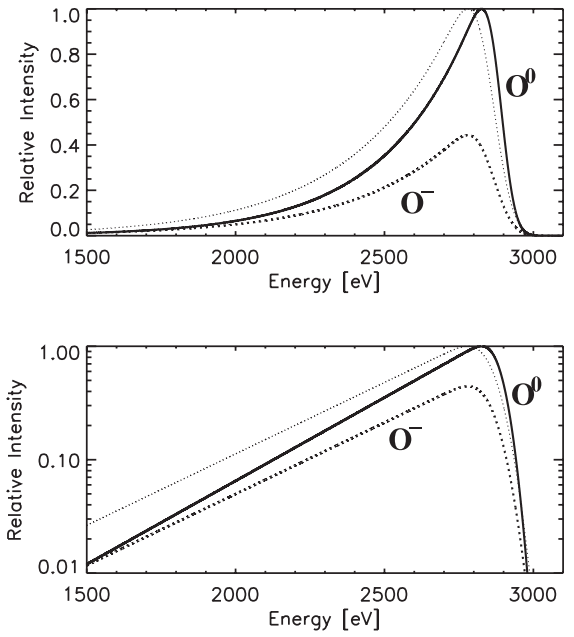

Fig. 8. Fits to the measured energy distributions for neutral (solid line) and negative (pointed line, thin pointed line: scaled to match neutrals) oxygen particles after reflection. The primary beam was a 3033 eV O^+ beam impinging on a $BaZrO_3$ surface at an incoming angle of about 5° as measured from the surface plane. The difference in energy loss upon scattering between neutrals and negative ions can be seen clearly.

They both end at the same maximum energy, which is clearly shown by the logarithmic plot in the lower panel, but the O^- distribution deviates from the O^0 distribution.

The angular scatters in azimuthal and polar directions were measured at the University of Bern and are shown in Fig. 9 for a 780 eV primary O_2^+ beam. It was 19° and 13° at FWHM in azimuthal and polar directions, respectively. We also calculated the reflection efficiency, i.e., the number of particles scattered inside the detection area divided by the total number of particles reflected from the sample. We obtained about 7%. The same measurement was performed some years ago and showed a much narrower scattering (10° and 7° at FWHM in azimuthal and polar directions), which can be seen in Fig. 10. The reflection efficiency was about 20% at that time, which shows that the sample was originally very smooth but it had suffered from experiments performed since then.

The positive charge state fractions for hydrogen, i.e., the fractions of positively charged particles in the reflected beam, were only measured at the University of Osnabrück. The results are plotted against primary energy per atom in Fig. 11. The data were corrected for the relative detection efficiency of the MSP detector at the particle energy. Primary H_2^0 (open circles), H_2^+ (filled circles) and H^+ (triangles) from ~300 to ~1500 eV were

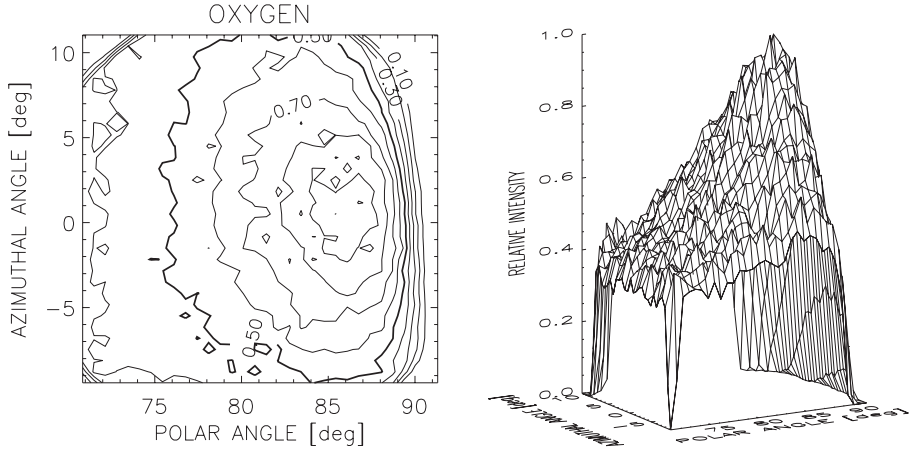

Fig. 9. Angular scattering for a 780 eV O_2^+ primary beam at 82° incidence angle (as measured from the surface normal) measured at the University of Bern, March 1999. The measured scatterings at FWHM are 19° and 13° in azimuthal and polar directions, respectively, and the reflection efficiency was about 7%.

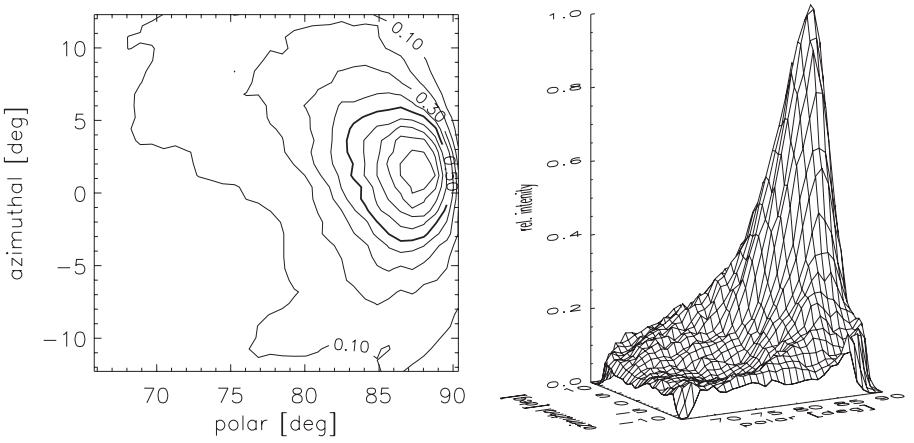

Fig. 10. Angular scattering for a 780 eV O_2^+ primary beam at 82° incidence angle (as measured from the surface normal) measured at the University of Bern some years ago shortly after sample preparation. The measured scatterings at FWHM were 10° and 7° in azimuthal and polar directions, respectively, and the reflection efficiency was about 20%.

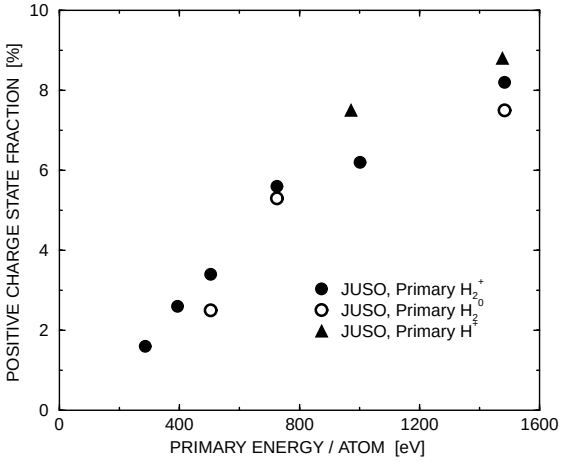

Fig. 11. Positive charge state fraction for hydrogen particles at 300–1500 eV per atom scattered off a $BaZrO_3$ surface at an incoming angle of about 5° as measured from the surface plane as a function of primary energy per atom. The positive ion fractions do not depend on whether we used primary H_2^+ (filled circles), primary H_2^0 (open circles) or primary H^+ (triangles) particles.

scattered off the $BaZrO_3$ sample. At 300 eV, only about 2% of the detected particles were positively charged, but this fraction increased with energy and at 1500 eV, we measured about 8% positive ions. The uncertainties of the JUSO results are higher than those of the Bern results because we had to consider the relative detection efficiency values at two very different energies (for the neutral particles and for the postaccelerated ions). The relative errors might amount to about 30% for energies below 1000 eV and become smaller with increasing energy because the relative detection efficiency curve flattens. Within the measurement uncertainties, we got the same fractions of positive ions using primary H_2^0, H_2^+ and H^+ particles.

The negative charge state fractions, i.e., the fractions of atoms or molecules that were negatively ionized upon reflection, were obtained from measurements at the University of Osnabrück and from experiments at the University of Bern. The two different sets of measurements were compared to each other.

Fig. 12 shows the negative charge state fractions for hydrogen plotted versus primary energy per atom. H_2^0 (open circles), H_2^+ (filled circles) and H^+ (triangles) at ~200–1500 eV primary energy per atom were produced in the JUSO apparatus and H_2^+ (squares) in the ILENA apparatus. Like the positive charge state fractions, the negative charge state fractions do not depend on the primary particle type. We found the same fractions of negative ions in the reflected beam for primary H_2^+, H_2^0 and H^+ particles. The measurements made with the ILENA apparatus were corrected for the different detection efficiencies for neutrals and ions,

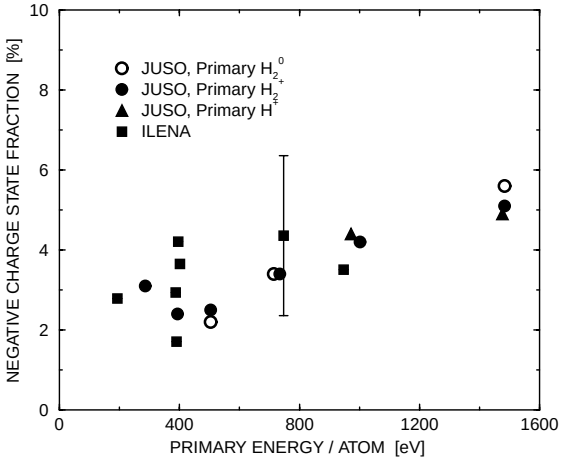

Fig. 12. Negative charge state fraction for hydrogen particles at 300–1500 eV per atom scattered off a $BaZrO_3$ surface at 82° (at the University of Osnabrück) and 78–87° (at the University of Bern) as measured from the surface normal as a function of primary energy per atom. The negative ion fractions do not depend on whether we used primary H_2^+ (filled circles), primary H_2^0 (open circles) or primary H^+ (triangles) particles. For primary H_2^+ we obtained the same results at the University of Osnabrück (JUSO apparatus) and at the University of Bern (ILENA apparatus). The two values obtained at 725 eV primary energy per atom for primary charged and neutral molecules are plotted at slightly different energies in order to make them both visible.

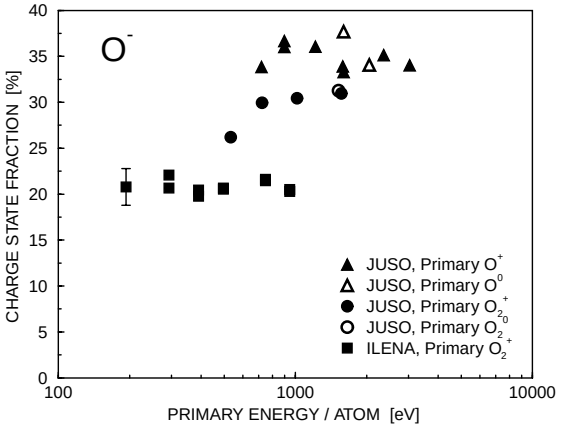

Fig. 13. Negative charge state fraction for oxygen particles at 500–3000 eV per atom scattered off a $BaZrO_3$ surface at 82° (at the University of Osnabrück) and 78–87° (at the University of Bern) as measured from the surface normal as a function of primary energy per atom. For primary O_2^+ we obtained different results at the University of Osnabrück (JUSO apparatus) and at the University of Bern (ILENA apparatus). The negative ion fractions were lower for primary molecules (circles, squares) than for primary atoms (triangles), but they do not depend on the charge state of the incoming particles (see open and filled symbols). The two values obtained at 1541 eV primary energy per atom for primary charged and neutral molecules are plotted at slightly different energies in order to make them both visible.

for the dissociation of the primary molecules, and for contamination of our negative ion signal by performing measurements with noble gases, which do not form negative ions [18,19]. The results obtained with the JUSO apparatus and the ILENA apparatus agree well with each other within the measurement uncertainties. We note that for the JUSO apparatus, the incidence angle with respect to the surface normal was about 85° given by the fixed scattering angle of 10°. For the ILENA apparatus, we varied the incidence angle from 78° to 87° and we did not observe a significant dependence of the negative charge state fraction on the incidence angle. The fraction of negatively charged hydrogen particles increases somewhat with energy. It is about 3% at 200 eV and reaches about 5% at 1500 eV. The estimated errors of the ILENA results are all approximately the same and are indicated just for a single data point for clearness of the figure.

As was mentioned above, we never detected any positive oxygen ions in the beam after reflection from our $BaZrO_3$ surface for primary energies in the range 1000–3000 eV (JUSO apparatus). The results for the negative charge state fraction plotted versus primary energy per atom are shown in Fig. 13. We scattered O^+ (filled triangles), O^0 (open triangles), O_2^+ (filled circles) and O_2^0 (open circles) off the $BaZrO_3$ surface in the JUSO apparatus and positive primary molecules in the ILENA apparatus, where we varied the incidence angle from 78° to 87° as we did for the hydrogen measurements. As can be seen from the Osnabrück results, the fraction of negative oxygen atoms in the reflected beam does not depend on whether the primary particles were neutral or positively charged. When using molecular primary particles, we found a negative ion fraction of about 22% in Bern and 26–31% in Osnabrück. For atomic primary beams we got about 35% negative ions. Moreover, we found constant negative charge

state fractions at the University of Bern, while those obtained at the University of Osnabrück increase slightly with energy.

4. Discussion

The negative charge state fractions for primary H_2^+ particles obtained at the two laboratories agreed well with each other. We also found from measurements with the JUSO apparatus that the measured fractions of negative and positive ions in the scattered beam did not depend on whether primary H_2^+, H_2^0, H^+ or H^0 were used. This suggests a complete memory loss of the incident particles. A complete memory loss of the incident charge state was reported for other projectile–target combinations, in particular for scattering ions off metal surfaces [6], and also for scattering oxygen particles off a semiconductor like silicon [20]. The memory loss can be explained by effective neutralization of the ions when approaching the surface. On the incoming trajectory, incident molecules could dissociate due to electronic excitation, resulting from capture of the neutralizing electron into an antibonding state. The measured fractions of positive and negative ions in the scattered particle flux are then most probably established on the outgoing trajectory.

When scattering O_2^+, O_2^0, O^+ and O^0 off the $BaZrO_3$ surface in the JUSO apparatus, we never found any positive ions or surviving molecules in the scattered beam. We found somewhat higher negative ion yields for primary atoms than for primary molecules. This might be due to an incomplete dissociation of the molecules before hitting the surface. Some molecules could dissociate only upon collisions with the surface atoms and the charge state of the outgoing particle will then depend on whether primary atomic or molecular particles were scattered because of their different electronic configurations. Since we did not observe any scattered oxygen molecules in our TOF spectra, we have to assume that they dissociate effectively on their way from the surface to the detector.

The lower ion yields for primary O_2^+ obtained with the ILENA apparatus compared to those obtained with the JUSO apparatus might be a consequence of the different residual pressures in the two vacuum chambers. In the ILENA apparatus, the pressure was about 10^{-7} mbar. This situation is what has to be expected onboard a satellite as the pressure inside an instrument will be of the same order. In the JUSO apparatus, the measurements were performed at a residual gas pressure of about 10^{-9} mbar. Though we heated the sample before performing measurements, it could be contaminated in the ILENA apparatus. Adsorbates could modify the surface band structure and thus affect the charge exchange process between projectile and surface. At the JUSO, we never observed any recoil atoms in the TOF spectra, which is a strong evidence that the surface was clean. Furthermore, the JUSO results suggest an increase of the negative oxygen ion fraction with energy while the respective ILENA values remained quite constant. At present, we are not able to give a good explanation about this difference. We considered the difference in the detection angle aperture (JUSO: $\pm 0.6°$; ILENA: $\pm 12.5°$ in azimuthal and polar directions) by dividing the position-resolved image recorded in the ILENA apparatus into subareas with respect to outgoing angle or specular reflection. According to our present understanding of the two experimental setups, the collection angle difference cannot account for the differences in the measured ion fractions but further measurements will be done to confirm this. We also considered in detail the electronic registration equipment at the two sites. Possibly, the different vacuum conditions can account for these differences. For data evaluation of a future space mission, it will be crucial to know the ionization efficiency as a function of energy. From the ionization efficiency together with the reflection efficiency and the energy loss one can, in principle, calculate the number of particles at a certain energy entering the instrument, i.e., the abundances of the species of interest in space.

Several theories exist for surface ionization. A study of negative ion formation upon reflection from low work function metal surfaces is given in [8] and explains the experimental results for low work function surfaces pretty well. When approaching a metal surface, the affinity level of an

atom undergoes a downshift and broadening close to the surface because of the interaction with the induced image charge in the metal. Once the position of the affinity level gets close to the Fermi level of the metal, resonant one-electron tunneling between the metal and the atom state will populate the negative ionic state. Since affinity levels of atoms are of the order of 1 eV, the work function of a metal (usually around 5 eV) has to be lowered by the application of a thin overlayer of an alkali metal or an alkali-earth metal to obtain appreciable yields of negative ions [6,10]. Unfortunately, we do not know the surface and volume band structure of the $BaZrO_3$ sample used for our measurements. But according to the constituent elements, the bonding will be, in part, covalent with a considerable ionic part. Thus, the binding energies of the valence band electrons will be much larger than about 1 eV, more likely around 5 eV, and there will also be a considerable bandgap, i.e., no empty electron states above the valence band, which could provide electrons for tunneling processes. The $BaZrO_3$ surface can therefore certainly not be treated like a free-electron metal.

During the past years also, theories for the formation of negative ions upon scattering off ionic crystals have been proposed. High ion yields and kinetic resonances for fast fluorine ions and atoms scattered off LiF(1 0 0) and KI(1 0 0) were found [21] and could be reasonably well described by the theory [22]. In [22], a binary encounter model is considered, where a valence electron can be transferred to the projectile as it interacts with an F^- anion. The energy difference between the initial state (before electron transfer) and the final state (after electron transfer) is calculated, taking into account the interaction between the ionized projectile and the hole left at the surface. The influence of the Madelung potential of the crystal on the negative ion leads to a considerable downshift of the affinity level of the projectile. The probability for a particle to be negatively charged on the outgoing trajectory increases with increasing effective number of binary collisions and thus, at grazing incidence angles. Recently, a theory based on the same binary encounter model has been proposed [23], which explains negative ion production from fluorine particles scattered off a MgO surface quite well. The authors [22,23] can explain the experimentally found high increase of the negative ion fraction with energy while the decrease at higher energies is not predicted by the current models as electron loss processes are not included. Electron loss processes for scattering off an insulator will be very different from the case of a metal target owing to the bandgap and possible surface states. The above models should work for ionic crystals in general. Kinetic resonances of negative charge state fractions have also been observed for oxygen and hydrogen scattered off a LiF(1 0 0) surface [24]. However, our results do not show any kinetic resonance in the investigated energy range (oxygen: 500–3000 eV per atom; hydrogen: 300–1500 eV per atom).

The results in [21] could also be qualitatively explained by a new theory [25]. The theory is developed from a Newns–Anderson Hamiltonian, whose parameters are chosen according to the surface and projectile. There is an effective band broadening of the solid's surface density of states as seen from the moving particle. When the parallel velocity is large enough so that the broadened and shifted affinity state overlaps with the extending valence band, the capture probability becomes different of zero. The capture probability decreases as soon as the electrons of the ion can populate the conduction band, which is also broadened as seen from the moving ion. The model predicts a strong dependence of the ionization probability on the parallel velocity of the moving ion, while the perpendicular velocity component has a smaller influence. As this model should work for metals as well as for semiconductors and insulators, our results seem to be in contrast to the predicted kinetic resonance. In our experiment, the parallel velocity component is proportional to the total particle velocity since the scattering angle remains constant. Thus a kinetic resonance related to parallel velocity should also appear when the data are plotted versus total energy. We only found small variations of the O^- and H^- fractions with energy when scattering oxygen and hydrogen particles off $BaZrO_3$.

The mean energy losses found for hydrogen and oxygen particles scattered off a $BaZrO_3$ surface are due to inelastic scattering. The elastic energy losses

upon binary collisions with a surface atom would not exceed about 1%. We measured a rather high energy loss compared to results reported in literature for other particles reflected from other clean surfaces [14,26,27]. This might be related to the high surface roughness of the $BaZrO_3$ sample used for this study.

The fact that the mean energy loss of hydrogen particles does not depend on whether we used primary H_2^+, H_2^0 or H^+ is consistent with the proposed complete dissociation and complete neutralization of the molecules on the incident particle trajectory. We note that in the interstellar gas and in the heliosphere, atomic particles are much more abundant than molecules, which means that the latter can be neglected. Hence, a memory loss of the initial particle state hardly affects data evaluation related to a future space mission.

The measured higher energy loss for negative oxygen ions compared to neutrals cannot be explained by current theories. The difference cannot be due to surface charging because the whole energy distribution of ions should then be shifted towards higher energies. As can be seen in Fig. 8, the curves of O^- and O^0 end at the same maximum energy but the shapes differ. Moreover, surface charging would also be observable when scattering hydrogen, which is not the case. We also considered the relative detection efficiency but it cannot account for the different energy distributions.

5. Conclusions

We measured high fractions (about 22–35%) of negative ions and no positive ions when scattering oxygen particles at 500–3000 eV primary energy per atom off a $BaZrO_3$ surface. When scattering hydrogen particles at 300–1500 eV per atom off the $BaZrO_3$ surface, about 3–5% of the particles were converted into negative ions and about 2–8% into positive ions. There is strong evidence for a complete memory loss of the incident charge state. Scattered hydrogen molecules dissociated almost completely (>99%) and we observed no surviving oxygen molecules. The variation of the ion fractions with energy will probably be small within an environment as present in a satellite instrument. The mean energy loss was proportional to the incident particle energy. We measured 12% for outgoing H^+, H^0 and H^-, 15% for O^0 and 18% for O^-.

We conclude that $BaZrO_3$ is a promising material for application on a space platform. It meets the most important requirements and seems better than AlN [12] concerning the conversion of hydrogen atoms.

Acknowledgements

The authors are grateful to Prof. P. Bochsler for continous support of this project. This work is supported by the Swiss National Science Foundation and by the Deutsche Forschungsgemeinschaft. K.S. thanks the Alexander-von-Humboldt-Stiftung for support.

References

[1] J. Geiss, M. Witte, Space Sci. Rev. 78 (1996) 229.
[2] T.E. Moore, D. Chornay, M.R. Collier, F.A. Herrero, J. Johnson, M.A. Johnson, J.W. Keller, J.F. Laudadio, J.F. Lobell, K.W. Ogilvie, P. Rozmarynowski, S.A. Fuselier, A.G. Ghielmetti, E. Hertzberg, D.C. Hamilton, R. Lundgren, P. Wilson, P. Walpole, T.M. Stephen, B.L. Peko, B. VanZyl, P. Wurz, J. Quinn, G.R. Wilson, Space Sci. Rev. 91 (2000) 155.
[3] P. Wurz, P. Bochsler, A.G. Ghielmetti, E.G. Shelley, F. Herrero, M.F. Smith, in: P. Varga, G. Betz (Eds.), Proceedings of the Symposium on Surface Science, Kaprun, Austria, 1993, p. 255.
[4] A.G. Ghielmetti, E.G. Shelley, S. Fuselier, P. Wurz, P. Bochsler, F. Herrero, M.F. Smith, T. Stephen, Opt. Eng. 33 (1994) 362.
[5] P. Wurz, M.R. Aellig, P. Bochsler, A.G. Ghielmetti, E.G. Shelley, S.A. Fuselier, F. Herrero, M.F. Smith, T.S. Stephen, Opt. Eng. 34 (1995) 2365.
[6] J.N.M. van Wunnik, J.J.C. Geerlings, E.H.A. Granneman, J. Los, Surf. Sci. 131 (1983) 17.
[7] J.J.C Geerlings, P.W. van Amersfoort, L.F.Tz. Kwakman, E.H.A. Granneman, J. Los, Surf. Sci. 157 (1985) 151.
[8] J. Los, J.J.C. Geerlings, Phys. Rep. 190 (1990) 133.
[9] N.D. Lang, Phys. Rev. B 4 (1971) 4234.
[10] C.F.A. van Os, P.W. Amersfoort, J. Los, J. Appl. Phys. 64 (1988) 3863.
[11] R. Schletti, P. Wurz, T. Fröhlich, Rev. Sci. Instr. 71 (2) (2000) 499.
[12] S. Jans, P. Wurz, R. Schletti, T. Fröhlich, J. Appl. Phys. 87 (5) (2000) 2587.

[13] P. Wurz, R. Schletti, M.R. Aellig, Surf. Sci. 373 (1997) 56.
[14] B. Willerding, H. Steininger, K.J. Snowdon, W. Heiland, Nucl. Instr. and Meth. B 2 (1984) 453.
[15] R. Yanochko, W. Brock, J. Krzanowski, J. Quinn, R.E. Leuchtner, in: Proceedings of the Mater. Res. Soc. Symposium, Boston, MA, December 1996, p. 1.
[16] K. Schmidt, T. Schlathölter, A. Närmann, W. Heiland, Chem. Phys. Lett. 200 (5) (1992) 465.
[17] B. Willerding, W. Heiland, K.J. Snowdon, Phys. Rev. Lett. 53 (21) (1984) 2031.
[18] R. Schletti, Master thesis, University of Bern, Switzerland, 1996.
[19] S. Jans, Master thesis, University of Bern, Switzerland, 2000.
[20] B. Hird, P. Gauthier, J. Bulicz, R.A. Armstrong, Phys. Rev. Lett. 67 (25) (1991) 3575.
[21] H. Winter, A. Mertens, C. Auth, A.G. Borisov, Phys. Rev. A 54 (3) (1996) 2486.
[22] A.G. Borisov, V. Sidis, Phys. Rev. B 56 (16) (1997) 10628.
[23] S.A. Deutscher, A.G. Borisov, V. Sidis, Phys. Rev. A 59 (6) (1999) 4446.
[24] H. Winter, C. Auth, T. Hecht, A. Mertens, Nucl. Instr. and Meth. B 157 (1999) 32.
[25] N. Lorente, J. Merino, F. Flores, M.Yu. Gusev, Nucl. Instr. and Meth. B 125 (1997) 277.
[26] J.I. Juaristi, A. Arnau, P.M. Echenique, C. Auth, H. Winter, Nucl. Instr. and Meth. B 157 (1999) 87.
[27] A. Närmann, Dissertation thesis, University of Osnabrück, Germany, 1989.